

RESEARCH

Open Access



miR390 family of *Cymbidium goeringii* is involved in the development of reproductive organs in transgenic *Arabidopsis*

Zihan Xu¹, Qian Liu¹, Yue Chen², Yuanhao He¹ and Fengrong Hu^{1*}

Abstract

Background: miR390s is an ancient family with a high level of conservation among plant miRNAs. Through the auxin signal transduction pathway, miR390 participates in diverse biological processes of plant growth and development. As an important Chinese traditional orchid, *Cymbidium goeringii* has unique flower shape and elegant fragrance. But its development has been greatly restricted because of the low flower bud differentiation and the difficult reproduction. This study aims to provide guidance for the role of cgo-miR390 in reproductive organ development to enhance the ornamental and economic value of *Cymbidium*.

Results: *MIR390a*, *MIR390b* and *MIR390c* of *C. goeringii* were cloned, and their length ranged from 130 to 150 nt. Each precursor sequence of cgo-miR390 contains 2 to 3 mature miRNAs. Three kinds of cgo-miR390s displayed distinct temporal and spatial expression patterns during floral development in *C. goeringii*. The overexpression of *MIR390s* alters morphology and function of stamens and pistils in *Arabidopsis*, such as enlargement of anther aspect ratio and separation of stylar and stigmas, which affects the development of fruits and seeds. In particular, the pollen amount decreased and the seed abortion rate increased in *cgo-MIR390c*-overexpressed plants.

Conclusions: cgo-miR390 family affected the development of reproductive organs in transgenic *Arabidopsis*. The study provides references for the genetic improvement for orchid with potentially great economic benefit.

Keywords: *Cymbidium goeringii*, miR390, Reproductive organ, Flower development, *Arabidopsis*

Background

MicroRNAs (miRNAs) are a class of non-coding endogenous small RNAs with 20–24 nucleotide (nt) in length [1], which have been identified as new regulators of gene expression at transcriptional, post-transcriptional and post-translational levels [2]. The ancient and highly conserved miRNA, miR390, plays an important role in diverse processes of plant growth and development, including apical dominance, leaf senescence, root formation and abiotic and biotic stress responses, through the

auxin signal transduction pathway. According to the miR-base database, miR390 family comprises no more than 4 members in most plants, such as only two members in *Arabidopsis thaliana* [3]. It has shown that some Auxin response factors (ARFs) are the target genes of miR390. Notably, miR390 triggers the production of trans-acting (ta) siRNAs from *TAS3* transcripts, which regulated ARFs in trans [4, 5].

miR390-*TAS3*-ARF regulatory network confers sensitivity and stability to auxin responses in various tissues and developmental stages. During root development, an auxin-response element (*AuxRE*) in the promoters of miR390 was bound by *ARF5/MONOPTEROS (MP)*, which affects the expression of miR390 in the transit-amplifying compartment of the root meristem. miR390

*Correspondence: hufengrong2003@sina.com

¹ College of Landscape Architecture, Nanjing Forestry University, 210037 Nanjing, Jiangsu Province, China

Full list of author information is available at the end of the article



© The Author(s) 2022. **Open Access** This article is licensed under a Creative Commons Attribution 4.0 International License, which permits use, sharing, adaptation, distribution and reproduction in any medium or format, as long as you give appropriate credit to the original author(s) and the source, provide a link to the Creative Commons licence, and indicate if changes were made. The images or other third party material in this article are included in the article's Creative Commons licence, unless indicated otherwise in a credit line to the material. If material is not included in the article's Creative Commons licence and your intended use is not permitted by statutory regulation or exceeds the permitted use, you will need to obtain permission directly from the copyright holder. To view a copy of this licence, visit <http://creativecommons.org/licenses/by/4.0/>. The Creative Commons Public Domain Dedication waiver (<http://creativecommons.org/publicdomain/zero/1.0/>) applies to the data made available in this article, unless otherwise stated in a credit line to the data.

then modulated the abundance of *ARF2/3/4* by *TAS3* [6]. miR390 was also specifically expressed at the sites of lateral root (LR) initiation where it triggers the biogenesis of ta-siRNAs to inhibit *ARF2/3/4*, and these ARFs affect auxin-mediated 390 accumulation as well [7, 8]. Therefore, an *ARF*-miR390-*TAS3* ta-siRNA-*ARF* regulatory network was established due to the positive and negative feedback regulation of miR390 by *ARF2/3/4*. In leaf development, it is likely that AGO associates with miR390 and cleaves *TAS3* precursor RNAs as ta-siRNAs. After *DCL4*-mediated processing, this complex cleaves their targets, including *ARF3* and *ARF4*, to regulate leaf morphology development in *Arabidopsis* [9–11]. Dissimilarly, the expression of miR390 in leaf polarity of maize is established and maintained independently of the ta-siRNA pathway [12]. In addition, miR390a has been previously reported to be involved in dark-induced leaf senescence, while *ARF2*, a target gene of miR390, positively regulated auxin-mediated leaf longevity in *Arabidopsis* [13–15].

Research in the floral development of miR390 is more limited. It has been reported that *TAS3* ta-siRNA, whose primary transcripts were processed by miR390, extended the juvenile phase and delayed the flowering phase through negative regulation of *ARF3* [16, 17]. Moreover, the analysis of miRNAs and degradome in four stages of fruit development, including young fruit stage, fruit expansion stage, fruit coloring stage, and full maturity stage, found that *TAS3a* and *TAS3b* were targeted and furtherly degraded by miR390 in tomato. LemiR390 showed a high level and negatively regulated the expression level of *LeTAS3* during the early stage, especially 1–2 weeks after flowering [18].

Taken together, miR390 plays critical roles in the regulation of plant growth and development, which can be used as a promising object for breeding and genetic

improvement in ornamental plants. Moreover, the effects of miR390 have been extensively studied in vegetative organs development, but less in reproductive organs. This is an innovative point in this study. As an important Chinese traditional orchid, *Cymbidium goeringii* has unique flower shape and elegant fragrance. But its development has been greatly restricted because of the low flower bud differentiation and the difficult reproduction. Here, we try to provide guidance for the role of a miRNA family in reproductive organ development. Recently, we obtained three predicted mature miR390s and their precursor sequences, designated cgo-miR390 family, from small RNA sequencing data in *C. goeringii*. This present study was aimed to investigate the expression patterns of miR390s in *C. goeringii* and their functional roles in *Arabidopsis*. The results suggest that cgo-miR390 family is a regulator involved in the development of reproductive organs in orchid plants.

Results

Sequence analysis of miR390s in *Cymbidium goeringii*

MIR390a, *MIR390b* and *MIR390c* sequences were identified based on the transcriptome sequence data. Then the three sequences were cloned from the leaf of *C. goeringii* ‘Songmei’, and their length ranged from 130 to 150 nt (Table S1). Sequencing results showed that these three cgo-*MIR390s* produced a total of 8 mature miRNAs, in which the sequence of 3 mature miRNAs each detected on *MIR390a* and *MIR390b* were identical (Table 1; Fig. 1 A). Predicted stem-loop structures of three precursor sequences were shown in Fig. 1, all of them had 2 nt overhang structure at the distal end of their arms, which resulted from *Dicer* cleavage [19]. According to reference [20], the minimal folding free energy indexes (MFEIs) of cgo-*MIR390a/b/c* were 1.00, 1.35 and 1.18, respectively. These calculation results indicated that the sequences

Table 1 List of gene information

Gene type	Gene name	Inclusion relation	Sequence length
Precursor sequences	cgo- <i>MIR390a</i>	●■▲	145bp
	cgo- <i>MIR390b</i>	●■▲	133bp
	cgo- <i>MIR390c</i>	●■	150bp
Mature miRNAs	cgo-miR390a-5p	●	21nt
	cgo-miR390b-5p	●	21nt
	cgo-miR390c-5p	●	21nt
	cgo-miR390a-3p.1	■	21nt
	cgo-miR390b-3p.1	■	21nt
	cgo-miR390c-3p	■	21nt
	cgo-miR390a-3p.2	▲	21nt
	cgo-miR390b-3p.2	▲	21nt

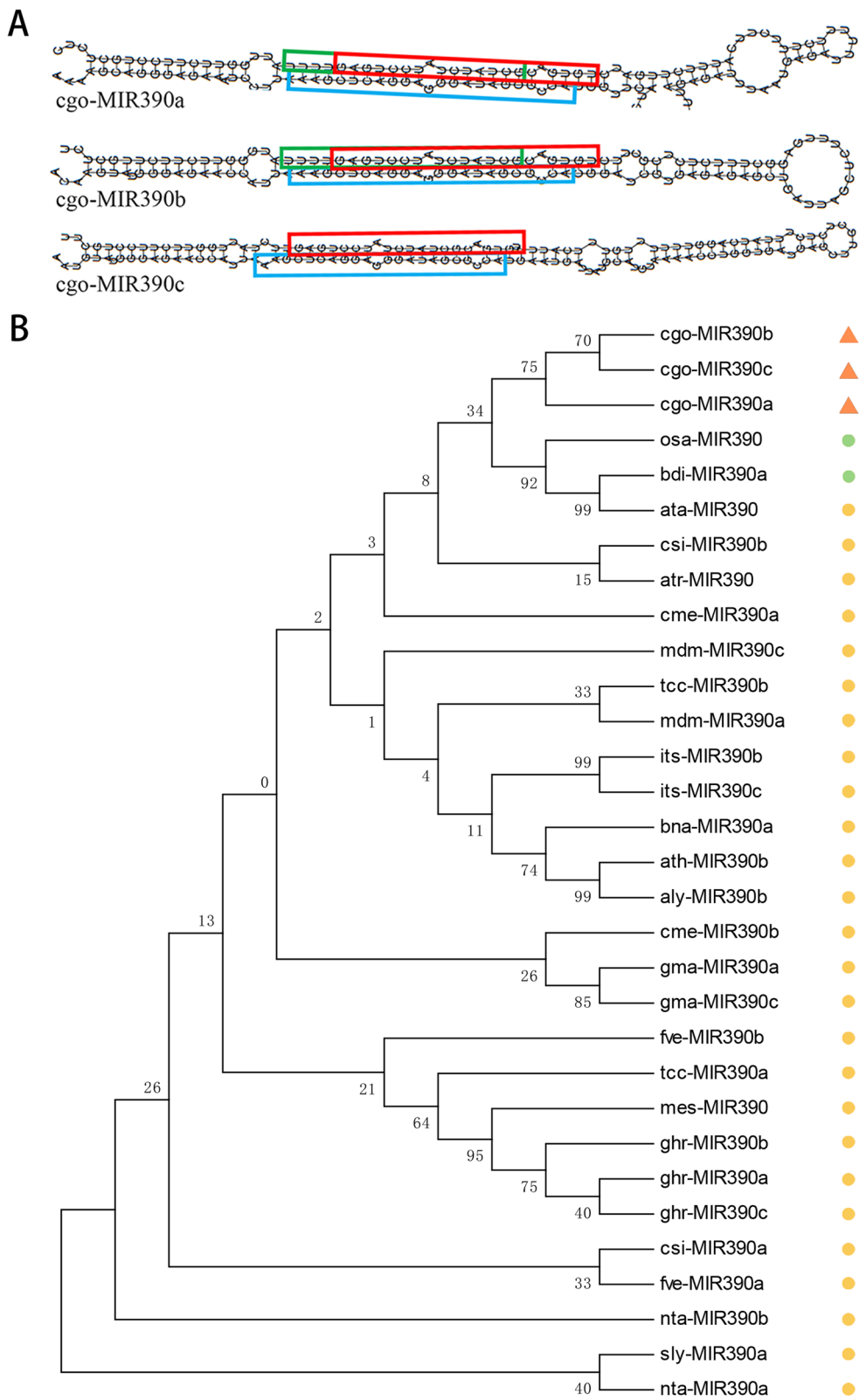


Fig. 1 Sequence analysis of *cgo-MIR390s*. **A** The secondary structures of *cgo-MIR390s* in *Cymbidium goeringii*. **B** The phylogenetic relationship of *cgo-MIR390s* with other homologous sequences. The triangles represent *C. goeringii*, the green dots represent monocotyledons, and the yellow dots represent dicotyledons

were all most likely to be miRNA due to the MFEIs were more than 0.85. In addition, no secondary stems or large loops interrupted the miRNA:miRNA* duplex, and there were fewer than 5 mismatched positions in duplex. These features are consistent with the universal characteristics of pre-miRNAs [21].

Analysis of homologous sequences found that three *MIR390* genes of *C. goeringii* showed strong homology, and all clustered together within the same branch of the phylogenetic tree (Fig. 1B). Furthermore, *MIR390s* in monocot plants display a higher sequence identity with *cgo-MIR390s* than those in dicots. It is obvious that this kind of pre-miRNA in monocot and dicot plants underwent evolutionary diversification. For analysis of mature miRNAs, *cgo-miR390a-5p* (*cgo-miR390b-5p*, *cgo-miR390c-5p*) was the most conserved one, followed by *miR390a-3p.1* (*miR390b-3p.1*, *miR390c-3p*) and *miR390a-3p.2* (*miR390b-3p.2*) (Fig. 2). This may be related to the evolution of *miR390* family in *C. goeringii* as well.

Expression analysis of *cgo-miR390s* in *Cymbidium goeringii*

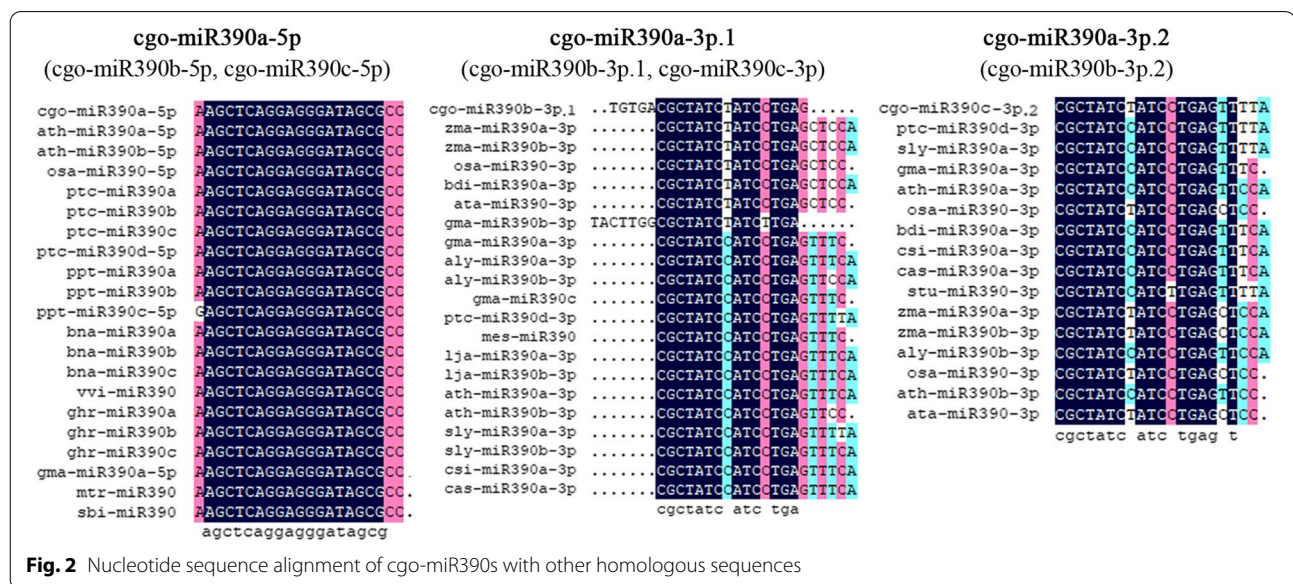
All three *miR390s* were expressed in each floral organ of fully open flowers. The expression of *cgo-miR390a-5p* was specific to the ovary (Fig. 3 A), whereas *cgo-miR390a-3p.1* was mainly expressed in lateral petal and stamen. By contrast, the expression of *cgo-miR390a-3p.2* was extremely low in all floral organs. During flower bud development, *cgo-miR390a-5p* and *cgo-miR390a-3p.1* had the highest expression when the flower bud length was 1-3 cm (Fig. 3B), while *cgo-miR390a-3p.2* has the lowest at that time. When the length of flower buds was 3-5 cm, these three *miR390s* were all expressed at

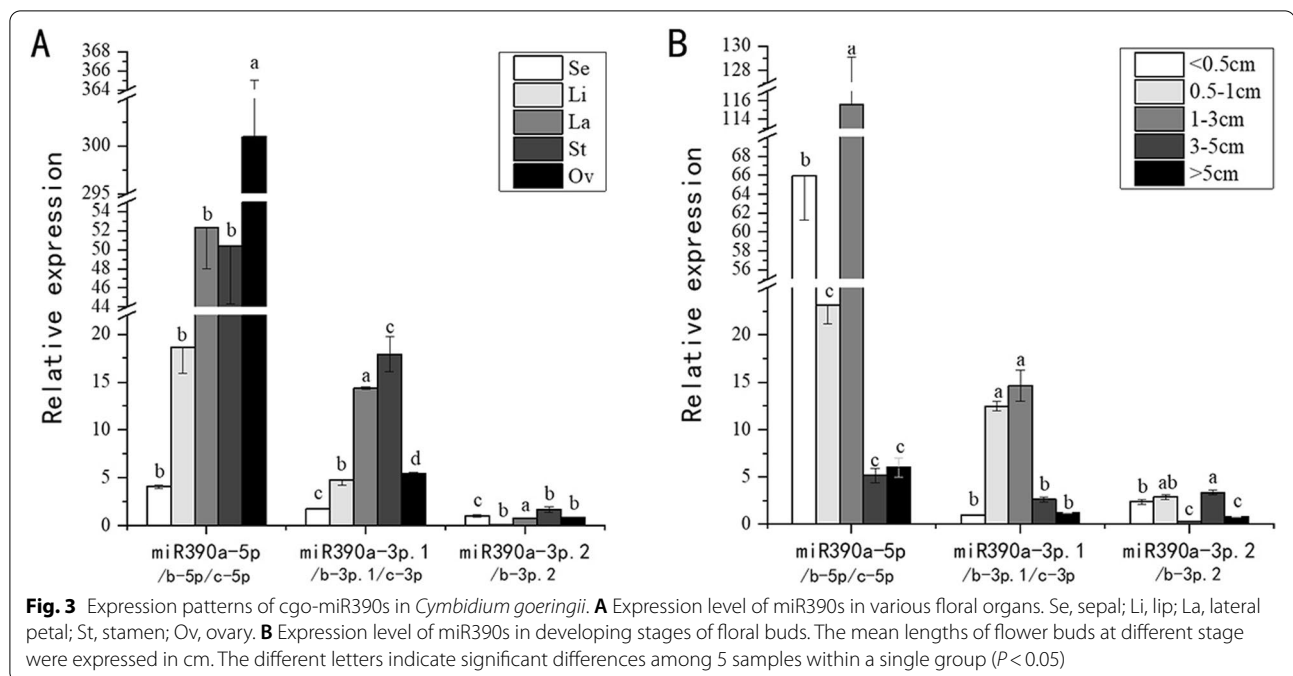
about the same level. These three kinds of *cgo-miR390s* showed overall non-overlapping expression patterns both temporally and spatially, which suggested they probably have functional divergence in regulating *Cymbidium* flower development (Fig. 3).

Effect of *cgo-miR390s* on stamens and pistils development in *Arabidopsis*

To investigate the function of *cgo-miR390* family in flower development, we overexpressed *cgo-MIR390s* in *Arabidopsis*. The flowering time of wild-type and transgenic plants was almost consistent (Fig. 4A). By observing the external morphology of fully open flowers, compared with wild-type (WT) plants, the pollen attached to the anthers of the three transgenic plants was less, which was most obvious in *cgo-MIR390c*-overexpressing *Arabidopsis* (Fig. 4B). We speculate that this might be due to anthers' early maturation, early dehiscence and insufficient pollen production.

Alexander staining was performed on the stamens of unopened flowers to further confirm this phenomenon. Figure 5 A showed that the anther aspect ratio (anther width/anther length) of three *cgo-MIR390s*-overexpressed plants was all larger than that of wild-type, suggesting that these three genes all regulated the morphological development of stamens. At this time, the pollen of wild-type did not reach full maturity. In contrast, pollen cells of *cgo-MIR390a* and *MIR390b* overexpressing plants were fully mature and kept inside the locules of anther, while the anther of *cgo-MIR390c*-overexpressing plants was prematurely dehisced and pollen grains were released (Fig. 5 A). Figure 5B-D also illustrated that the pollen amount from fully open flowers of





cgo-MIR390s-overexpressed plants, especially *MIR390c*, was lower than the wild-type, but the pollen viability was generally as high as that of WT. Moreover, in vitro pollen germination assays showed normal pollen germination and pollen tube growth in transgenic plants (Fig. 5E-G).

The pistil morphologies also changed in transgenic *Arabidopsis*, mainly in the stigma. Figure 5 H showed that the stigma papilla cells of wild-type plants exhibited a finger-like shape and were tightly arranged, while the majority of papilla cells of *cgo-MIR390a* and *MIR390b* overexpressed plants are shrunken. This kind of cells of *MIR390c*-overexpressed plants displayed morphology similar to the wild-type but was more loosely arranged. In addition, all transgenic plants split styles and stigmas. These changes in stamens and pistils may affect fruit development and seed setting rate.

Effect of cgo-miR390s on fruits and seeds development in *Arabidopsis*

Although all transgenic plants flowered at a similar time as the wild-type, their senescence time was earlier than WT, especially in the reduced flowering (Fig. 6) and fruit ripening time (Fig. 7 A). By observing under a stereomicroscope, the fruit pods of all transgenic plants were thicker than those of the wild-type, with those of *cgo-MIR390a* and *MIR390b* overexpressed plants longer than *MIR390c* and WT (Fig. 7 A and B). The anatomical observation of fruits was further performed, which showed that the three genes overexpressed plants had different degrees of ovule abortion, and the seed volume

of transgenic plants was larger than that of WT (Fig. 7 C). These results further indicated that *cgo-miR390s* were involved in fruit development by regulating the development of floral organs.

Discussion

miR390s in plants are the ancient family of miRNAs with a high level of conservation among species [22]. Mature sequence analysis indicated that the three kinds of miR390s in *Cymbidium goeringii* were conserved. Secondary structure prediction showed that the mature miRNAs were all clustered in the same precursor. Studies of miRNA clusters in animals showed that evolutionarily conserved miRNAs are significantly enriched in clusters. The miRNAs in the same cluster have cooperative effects, which is called “functional co-adaptation” model [23]. We then analyzed the expression patterns by Quantitative real-time PCR (qRT-PCR), observing that the expression levels of *cgo-miR390a-5p* (*miR390b-5p*, *miR390c-5p*) and *cgo-miR390a-3p.1* (*miR390b-3p.1*, *miR390c-3p*) were opposite in ovary but the expression trends of them in other floral organs were similar. During floral buds development, the highest expression of *cgo-miR390a-5p* and *cgo-miR390a-3p.1* was obtained when the floral buds grew to 1-3 cm and significantly decreased after this stage. In particular, the expression pattern of *miR390a-3p.2* (*miR390b-3p.2*) was different from the other two kinds of *cgo-miR390s* not only in floral organs but also in floral bud development. The above results indicated that there may be synergy between *cgo-miR390a-5p* and



Fig. 4 **A** Flowering time observation of wild type and transgenic *Arabidopsis* plants. **B** Flower characterization of wild type and transgenic *Arabidopsis* plants. The first line showed the top view of flowers and the second line showed the side view of flowers under a stereomicroscope

cgo-miR390a-3p.1, while *miR390a-3p.2* were inclined to play roles independently. These inferences seemed to be further substantiated by the functional verification in *Arabidopsis*.

The overexpressed plants of *cgo-miR390s* cluster showed similar phenotypes in some of the organs, such as pod thickening, anther aspect ratio enlargement, and seed abortion. Moreover, the similarity of functions between *cgo-MIR390a* and *cgo-MIR390b* was more clear, while the phenotypes of *cgo-MIR390c*-overexpressed plants were different. This might be caused by the lack of a mature miRNA in *cgo-MIR390c*, which needs to

be validated by further experiments. Of course, there are some differences between *cgo-MIR390a* and *cgo-MIR390b* as well, such as the effect on pods morphology. Although both *cgo-MIR390a* and *MIR390b* produce mature miRNAs, the stem-loop structure and precursor sequences between them were all different. In addition, the expression of mature miRNAs was not linearly associated with that of precursor miRNAs, which might be regulated at several levels [24]. These might be the reasons for their functional difference.

Next, how *cgo-miR390s* is involved in the regulation of reproductive organs development remains an open

(See figure on next page.)

Fig. 5 Phenotype changes in floral organs of wild type and transgenic *Arabidopsis* plants. **A** The stamens staining with Alexander solution under an optical microscope. **B** The pollen grains staining with Alexander solution under an optical microscope. **C–D** The statistical results of the pollen stains' number and staining rate under an optical microscope with 10× magnification. **E** In vitro pollen germination and pollen-tube growth under an optical microscope with 20× magnification. **F–G** The statistical results of pollen germination rate and pollen tubes' length. **H** The stigma of pistils under an electron microscope. The different letters indicate significant differences ($P < 0.05$)

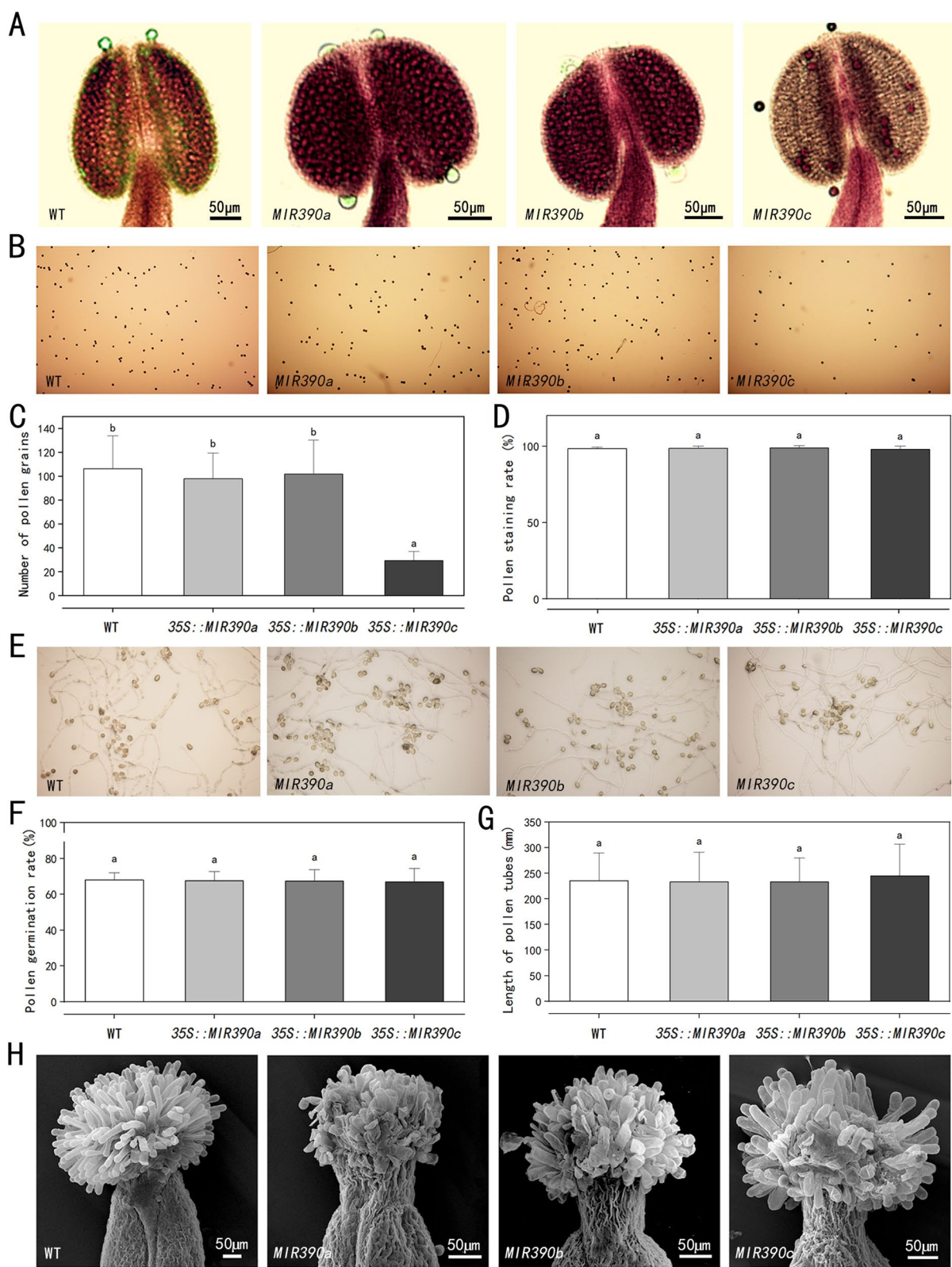


Fig. 5 (See legend on previous page.)

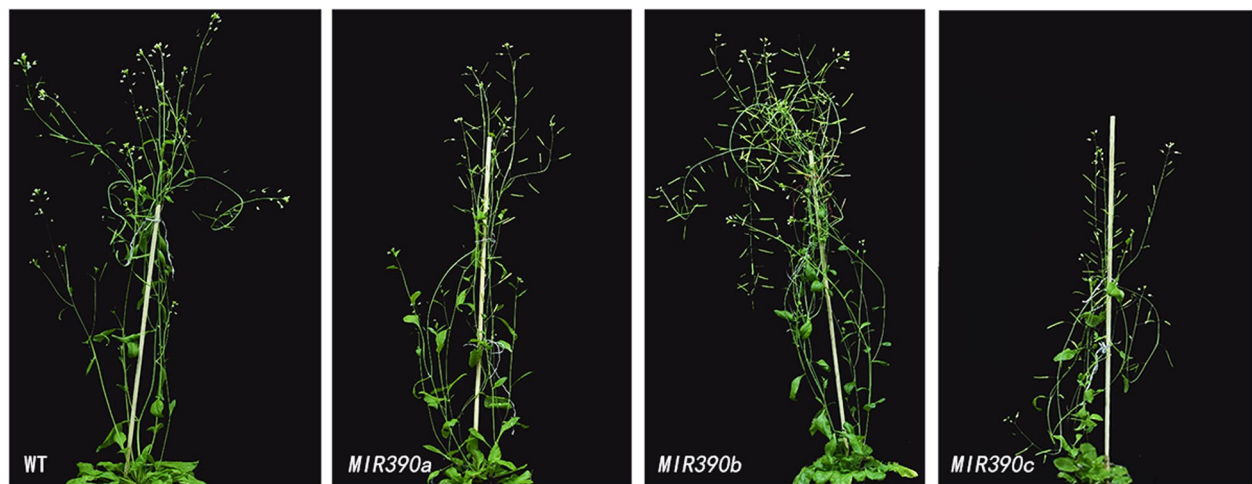


Fig. 6 Fruit ripening observation of wild type and transgenic *Arabidopsis* plants

question, but we offer some possibilities. Existing studies indicated that miR390s play a potential role in the anther development and regulation of male-sterility in tomato, which was similar to the results in our study. The researchers speculated that it might be related to *TasiARFs*, even though their regulatory mechanisms are poorly understood [25]. In *Arabidopsis*, the miR390-*TAS3-ARF2/3/4* regulatory network is an integral part of the regulatory networks mediating auxin response [6, 26]. Flower phenotypes of *arf2* mutants showed infertility of the early-produced flowers, which was probably caused by the early elongation of gynoecium [27]. *TEX1*- and *TAS3*-mediated restriction of *ARF3* expression limits excessive megaspore mother cell formation [28]. The overexpressed plant of *cgo-MIR390c* seems to show a tendency towards these phenotypes. Moreover, the *ETT/ARF3* mutant exhibited some developmental abnormalities such as an expansion of the stylar and stigmatic regions [29]. Seed size and weight were dramatically increased in an *AtARF2* mutant [30]. These were very similar to all *cgo-miR390s*-overexpressed plants. Notably, three *cgo-MIR390s* overexpressed plants exhibited different degrees of ovule abortion, but Alexander staining and in vitro pollen germination assays showed that the pollen collected from transgenic *Arabidopsis* had normal viability. Therefore, we speculated that the ovule abortion of transgenic plants could result from aberrant development of female reproduction, such as stigma defect shown in Fig. 5 H, transmission tract defect and/or female gametophyte defects [31]. Of these, failed fertilization in *cgo-MIR390c*-overexpressed plants may also be caused by premature release of pollen grains. In addition, the miR390-*TAS3-ARF* pathway was also involved in other biological processes of non-model plants like the

response to salt stress [32]. But this functionally important and archetypal regulatory pathway in land plants occurred significant variation [33]. All of these have brought more light to the verification experiments of target genes and the regulatory mechanism of *cgo-miR390s* in reproductive organs.

Conclusions

In conclusion, *cgo-miR390* family plays important roles in the reproductive organs of plants. Three kinds of *cgo-miR390s* displayed distinct temporal and spatial expression patterns during floral development in *Cymbidium goeringii*. The results also demonstrate that the overexpression of *MIR390s* alters the morphology and function of stamens and pistils in *Arabidopsis*, which affects the development of fruits and seeds. These findings preliminarily reveal the functions of *cgo-miR390s* and suggest that they can potentially be used for genetic improvement for orchid.

Methods

Plant materials and growth conditions

The Songmei cultivar of *C. cymbidium* was cultivated in a naturally lit glasshouse in the Institute of Horticulture, Zhejiang Academy of Agricultural Sciences (Hangzhou, Zhejiang, China). The *Arabidopsis* variety Columbia (Col-0) was used for gene overexpression and was grown at (22 ± 1) °C, 16 h day/8 h night in an artificial climate chamber.

Extraction of RNA and qRT-PCR analysis

Total small RNA was extracted from the plants using MiniBEST Universal RNA Extraction Kit (Takara, Dalian, China). The total small RNA was then reverse transcribed into cDNA using miRNA 1st Strand cDNA Synthesis

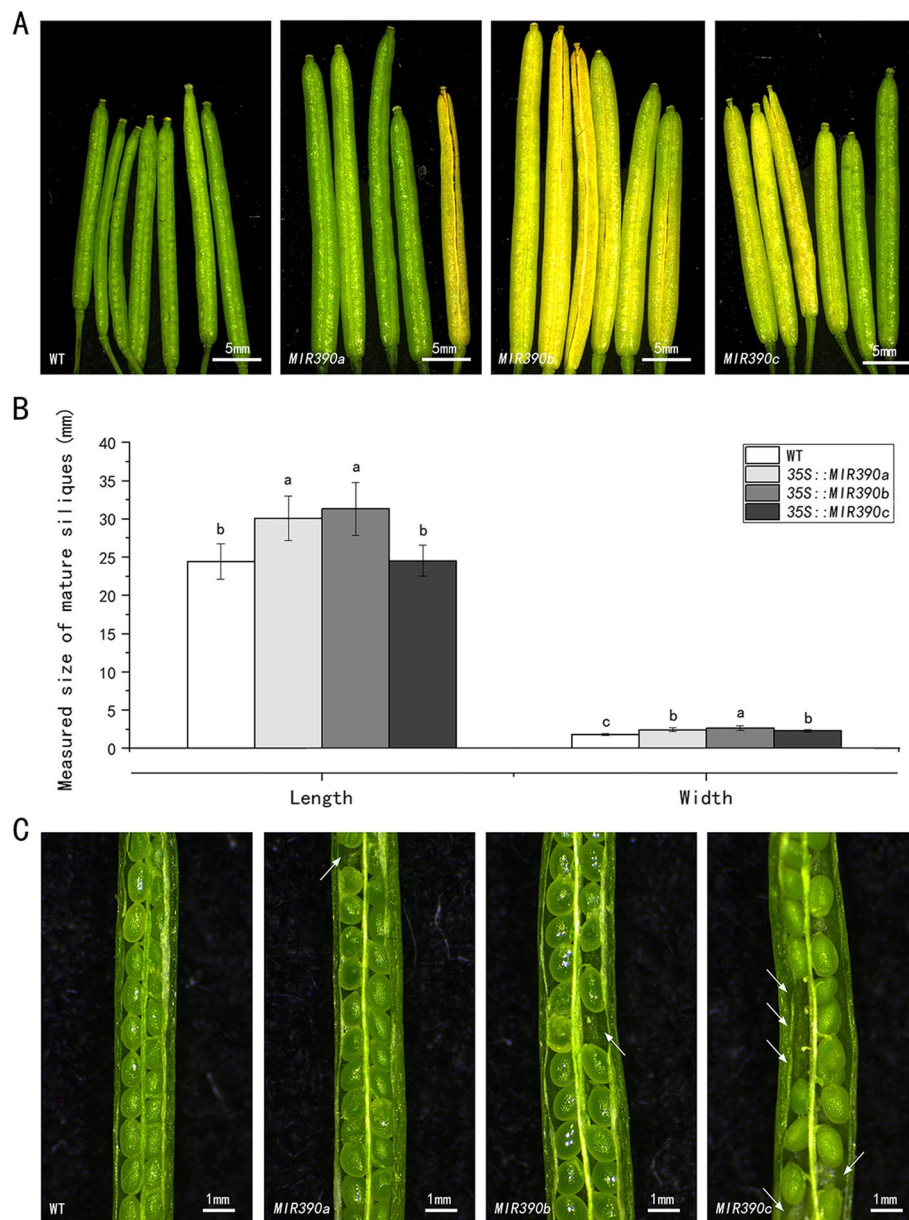


Fig. 7 Phenotype changes in fruit pods of wild type and transgenic *Arabidopsis* plants. **A** Comparison of fruit morphology. **B** Measured size of mature siliques. The different letters indicate significant differences among 4 samples within a single group ($P < 0.05$). **C** Anatomical images of fruit pods. The white arrows point to absent or abort seeds

Kit (Vazyme, Nanjing, China) with stem-loop primer. qRT-PCR reaction solution was configured according to the instruction of ChamQ Universal SYBR qPCR Master Mix (Vazyme, Nanjing, China), and the action was performed using a StepOnePlus real-time PCR system (ThermoFisher, Waltham, USA) under the following conditions: polymerase activation at 95°C for 5 min, followed by 40 cycles at 95°C for 15s and 60°C for 1 min. We used 18 S rRNA and U6 as internal reference genes for

C. goeringii and *Arabidopsis*, respectively. The threshold cycle (Ct) values of the PCR were averaged, and the relative transcript levels were quantified using the $2^{-\Delta\Delta C_t}$ method. The sequences of all the primers for this experiment are shown in Table 2.

Cloning of cgo-miR390 family and bioinformatic analysis

The putative precursors of cgo-miR390 family, *MIR390a* (145 bp), *MIR390b* (133 bp), and *MIR390c*

Table 2 List of primers sequences used for the experiments

Sequence type	Gene name	Primer sequences
Precursor cloning	<i>cgo-MIR390a</i>	F: gagaacacgggggactctagaAAAAGCAGGGAGAAATCCTTAAAG R: ataagggactgaccacccgggGAGAGCAGGAAGAACCAATAAACT
	<i>cgo-MIR390b</i>	F: gagaacacgggggactctagaACAAGTATGGGAGAACCATTAAAGC R: ataagggactgaccacccgggAAGAGCAAGAAGAACCCATAAACTC
	<i>cgo-MIR390c</i>	F: gagaacacgggggactctagaAATGTATGGGAGAACCATTAAAGCT R: ataagggactgaccacccgggAGAGCAGGAAGAACCAATAGAACTCA
Reverse transcription	<i>cgo-miR390a-5p</i>	GTCGTATCCAGTGCAGGGTCCGAGGTATTCGACTGGATACGACTGGCGC
	<i>cgo-miR390a-3p.1</i>	GTCGTATCCAGTGCAGGGTCCGAGGTATTCGACTGGATACGACTCAGG
	<i>cgo-miR390a-3p.2</i>	GTCGTATCCAGTGCAGGGTCCGAGGTATTCGACTGGATACGACAAACT
Fluorescence quantification	<i>cgo-miR390a-5p</i>	F: CGCGAAGCTCAGGAGGGATA R: AGTGCAGGGTCCGAGGTATT
	<i>cgo-miR390a-3p.1</i>	F: GCGCGTGTGACGCTATCTAT R: AGTGCAGGGTCCGAGGTATT
	<i>cgo-miR390a-3p.2</i>	F: CGCGCGGCTATCTATCCTG R: AGTGCAGGGTCCGAGGTATT
	18S	F: GGTCTATTGTGTGGCT R: TCGCAGTGTTCTGCTCT
	U6	F: GGTGCTAAGAAGAGGAAGAAT R: CTCCTCTTCTGGTAAACGT

(150 bp), were amplified with the primer pairs listed in Table 2, and then cloned into pBI121 vector at double restriction sites (*XbaI* and *SmaI*) to construct into recombinant vector. Gene amplification was performed by a standard PCR procedure, and the annealing temperatures were all 60 °C.

Secondary structure and minimum free energy (MFE) prediction were performed with the online tool RNAfold (<http://rna.tbi.univie.ac.at/>). Homologous sequence of precursors and matures were download from miRbase (<http://www.mirbase.org/index.shtml>), and then aligned in DNAMAN 8.0 software. The phylogenetic tree was constructed using MEGA 6.0 with the neighbor joining (NJ) method.

Transformation into Arabidopsis

pBI121-35 *S::MIR390a*, pBI121-35 *S::MIR390b* and pBI121-35 *S::MIR390c* were transformed into *Arabidopsis* Col-0 by the *Agrobacterium tumefaciens*-mediated floral dipping method [34]. T₀ seeds were screened on MS media containing 50 mg L⁻¹ kanamycin to obtain T₁ plants, and the gene insertions were confirmed by detection of genomic DNA PCR (Fig. S1). T₂ plants were obtained through phenotypic observation and gene expression measurement. Screening was performed until homozygous lines of T₃ generation were obtained.

In vitro pollen germination and pollen-tube growth

Pollen was collected from fully open flowers and germinated on *Arabidopsis thaliana* pollen medium according to the procedure of Fan et al. [35] with minor modifications. This medium consisted of 1mM KCl, 10mM CaCl₂, 0.8mM MgSO₄, 1.5mM boric acid, 10 mg/L myo-inositol, 5mM Mes, 18% (w/v) sucrose and 1.0% (w/v) agarose. And the pH was adjusted to 5.8 using Tris-hydroxymethyl aminomethane (Tris) base. Pollen germination was determined by microscopy after 10 h incubation in a chamber at 25 °C and 100% relative humidity. The pollen grains were recorded as germinated when the pollen tube length was equal to or greater than the pollen grain diameter, as described by Boavida and McCormick [36].

Alexander staining of stamens and pollen

For examination of stamen samples, the stamens were collected from flowers that were about to bloom, when the anthers had not yet split but the pollens were mature. The stamens were fixed in Alexander stain solution (Jis-skang, Qingdao, China) at 55°C for 3 h, and observed under the optical microscope.

For examination of pollen samples, 30 fully open flowers were randomly collected from the plants and mixed with ddH₂O in a 1.5 mL centrifuge tube by vortex for 2 min, then took the flowers out. After centrifugation at 11,000 rpm for 1 min (at room temperature), the

supernatant was discarded. The pollen precipitation was fixed in Alexander stain solution at 55°C for 3 h. Then the morphology of pollen was observed under a microscope, and the number, coloration rate and aberration rate of pollen were counted.

Scanning electron microscopy (SEM)

The pistils collected from fully open flowers were infiltrated in 4% glutaraldehyde (Electron Microscopy China, Beijing, China) overnight. Samples were dehydrated in an ethanol series, dried by EMITECH-K850 (Quorum, Hertfordshire, England) and sputter coated with Platinum. Images were taken with a Quanta 200 Scanning Electron Microscope (FEI, Hillsboro, USA) at an accelerating voltage of 25 kV.

Abbreviations

miRNA: MicroRNA; Nt: nucleotide; ARF: Auxin response factor; ta: Trans-acting; AuxRE: Auxin-response element; MP: MONOPTEROS; LR: Lateral root; Se: Sepa; Li: Lip; La: Lateral petal; St: Stamen; Ov: Ovary; WT: Wild-type; qRT-PCR: Quantitative real-time PCR; Col: Columbia.

Supplementary Information

The online version contains supplementary material available at <https://doi.org/10.1186/s12870-022-03539-3>.

Additional file 1.

Additional file 2.

Additional file 3.

Additional file 4.

Additional file 5.

Additional file 6.

Additional file 7.

Additional file 8.

Acknowledgements

Not application.

Plant ethics

Experimental research and field studies on plants (either cultivated or wild), including the collection of plant material are conducted in compliance with relevant institutional, national, and international guidelines and legislation.

Authors' contributions

ZX and QL conducted the experiments, analyzed the data and wrote the manuscript. ZX and YH edited the manuscript. YC and FH designed the experiments and edited the manuscript. All authors read and approved the manuscript.

Funding

This work was funded by the Postgraduate Research & Practice Innovation Program of Jiangsu Province (KYCX21_0928) and the University Brand Major Construction Foundation of Jiangsu Province (PPZY2015A063). The funders had no role in study design, data collection and analysis, decision to publish, or preparation of the manuscript.

Availability of data and materials

All data generated or analyzed during this study are included in this published article and its supplementary information files. The precursor sequences and mature miRNAs of cgo-miR390s described here are available in the Supplemental Files and at Genbank: OM824433-OM824435.

Declarations

Ethics approval and consent to participate

There are no ethical issues involved.

Consent for publication

Not applicable.

Competing interests

The authors declare that they have no competing interests.

Author details

¹College of Landscape Architecture, Nanjing Forestry University, 210037 Nanjing, Jiangsu Province, China. ²Institute of Horticulture, Zhejiang Academy of Agricultural Sciences, 310021 Hangzhou, Zhejiang Province, China.

Received: 16 August 2021 Accepted: 15 March 2022

Published online: 26 March 2022

References

- Rogers K, Chen XM. Biogenesis, turnover and mode of action of plant microRNAs. *Plant Cell*. 2013;25:2383–99.
- Fan K, Fan DM, Ding ZT, et al. Cs-miR156 is involved in the nitrogen form regulation of catechins accumulation in tea plant (*Camellia sinensis* L.). *Plant Physiol Biochem*. 2015;97:350–60.
- Gustafson AM, Allen E, Givan S, et al. ASRP: the *Arabidopsis* small RNA project database. *Nucleic Acids Rec*. 2005;33:D637–40.
- Gustafson A, Gustafson C, Carrington J, et al. microRNA-directed phasing during trans-acting siRNA biogenesis in plant. *Cell*. 2005;121:207–21.
- Seo E, Kim K, Park JH, et al. Genome-wide comparative analysis in Solanaceous species reveals evolution of microRNAs targeting defense genes in *Capsicum* spp. *DNA Res*. 2018;25(6):561–75.
- Dastidar MG, Scarpa A, Mägele I, et al. ARF5/MONOPTERIS directly regulates miR390 expression in the *Arabidopsis thaliana* primary root meristem. *Plant Direct*. 2019;3(2):e00116.
- Martin E, Jouannet V, Herz A, et al. miR390, *Arabidopsis* TAS3 tasiRNAs, and their *AUXIN RESPONSE FACTOR* targets define an autoregulatory network quantitatively regulating lateral root growth. *Plant Cell*. 2010;22:1104–17.
- Yoon EK, Yang JH, Lim J, et al. Auxin regulation of the microRNA390-dependent transacting small interfering RNA pathway in *Arabidopsis* lateral root development. *Nucleic Acid Rec*. 2010;38(4):1382–91.
- Adenot X, Elmayan T, Lauressergues D, et al. DRB4-dependent TAS3 trans-acting siRNAs control leaf morphology through AGO7. *Curr Biol*. 2006;16:927–32.
- Montgomery TA, Howell MD, Cuperus JT, et al. Specificity of ARGO-NAUTE7-miR390 interaction and dual functionality in TAS3 trans-acting siRNA formation. *Cell*. 2008;133:128–41.
- Endo Y, Iwakawa H, Tomari Y, et al. *Arabidopsis* ARGONAUTE7 selects miR390 through multiple checkpoints during RISC assembly. *EMBO Rep*. 2013;14(7):652–58.
- Nogueira FTS, Chitwood DH, Madi S, et al. Regulation of small RNA accumulation in the maize shoot apex. *PLoS Genet*. 2009;5(1):e1000320.
- Osborne DJ. Control of leaf senescence by auxins. *Nature*. 1959;183(4673):1459–60.
- Lim PO, Lee IC, Kim J, et al. Auxin response factor 2 (ARF2) plays a major role in regulating auxin-mediated leaf longevity. *J Exp Bot*. 2010;61(5):1419–30.
- Huo XY, Wang C, Teng YB, et al. Identification of miRNAs associated with dark-induced senescence in *Arabidopsis*. *BMC Plant Biol*. 2015;15:266.
- Garcia D. A miRacle in plant development: role of microRNAs in cell differentiation and patterning. *Semin Cell Dev Biol*. 2008;19(6):586–95.

17. Fahlgren N, Montgomery TA, Howell M, et al. Regulation of AUXIN RESPONSE FACTOR3 by TAS3 ta-siRNA affects developmental timing and patterning in *Arabidopsis*. *Curr Biol*. 2006;16(9):939–44.
18. Yu LL, Liu WW, Fang Y, et al. Identification and expression character analysis of LemIR390 and its potential target *LeTAS3* in tomato. *Acta Horticulturae Sinica*. 2015;42(2):271–79.
19. Blaszczyk J, Tropea JE, Bubunenko M, et al. Crystallographic and modeling studies of RNase III suggest a mechanism for double-stranded RNA cleavage. *Structure*. 2001;9:1225–36.
20. Zhang BH, Pan XP, Cox SB, et al. Evidence that miRNAs are different from other RNAs. *Cell Mol Life Sci*. 2006;63:246–54.
21. Axtell MJ, Meyers BC. Revisiting criteria for plant microRNA annotation in the era of big data. *Plant Cell*. 2018;30:272–84.
22. Yang CX, Xu M, Wang MX, et al. Advance on miR160/miR167/miR390 family and its target genes in plants. *Journal of Nanjing Forestry University (Natural Sciences Edition)*. 2014;38(3):155–59.
23. Wang YR, Luo JJ, Zhang H, et al. microRNAs in the same clusters evolve to coordinately regulate functionally related genes. *Mol Biol Evol*. 2016;33(9):2232–47.
24. Zhang JH, Zhang SG, Wu T, et al. Expression analysis of five miRNAs and their precursors during somatic embryogenesis in larch. *Chin Bull Bot*. 2012;47:462–73.
25. Omidvar V, Mohorianu I, Dalmay T, et al. Identification of miRNAs with potential roles in regulation of anther development and male-sterility in *7B-1* male-sterile tomato mutant. *BMC Genomics*. 2015;16:878.
26. Williams L, Carles CC, Osmont KS, et al. A database analysis method identifies an endogenous trans-acting short-interfering RNA that targets the *Arabidopsis* *ARF2*, *ARF3*, and *ARF4* genes. *P Natl Acad Sci USA*. 2005;102(27):9703–8.
27. Okushima Y, Mitina I, Quach HL, et al. AUXIN RESPONSE FACTOR 2 (ARF2): a pleiotropic developmental regulator. *Plant J*. 2005;43:29–46.
28. Su ZX, Zhao LH, Zhao YY, et al. The THO complex non-cell-autonomously represses female germline specification through the *TAS3-ARF3* module. *Curr Biol*. 2017;27(11):1597–609.
29. Sessions RA, Zambryski PC. *Arabidopsis* gynoecium structure in the wild type and in *ettin* mutants. *Development*. 1995;121:1519–32.
30. Schruff MC, Spielman M, Tiwari S, et al. The *AUXIN RESPONSE FACTOR 2* gene of *Arabidopsis* links auxin signalling, cell division, and the size of seeds and other organs. *Development*. 2006;133(2):251–61.
31. Makkena S, Lee E, Sack FD, et al. The R2R3 MYB transcription factors FOUR LIPS and MYB88 regulate female reproductive development. *J. Exp. Bot*. 2012;63(15):5545–58.
32. Wen FL, Yue Y, He TF, et al. Identification of miR390-TAS3-ARF pathway in response to salt stress in *Helianthus tuberosus* L. *Gene*. 2020;738:144460.
33. Xia R, Xu J, Meyers BC, et al. The emergence, evolution and diversification of the miR390-TAS3-ARF pathway in land plants. *Plant Cell*. 2017;29(6):1132–47.
34. Clough SJ, Bent AF. Floral dip: a simplified method for *Agrobacterium*-mediated transformation of *Arabidopsis thaliana*. *Plant J*. 1998;16(6):735–43.
35. Fan LM, Wang YF, Wang H, et al. In vitro *Arabidopsis* pollen germination and characterization of the inward potassium currents in *Arabidopsis* pollen grain protoplasts. *J Exp Bot*. 2001;52(361):1603–14.
36. Boavida LC, McCormick. Temperature as a determinant factor for increased and reproducible in vitro pollen germination in *Arabidopsis thaliana*. *Plant J*. 2007;52:570–82.

Publisher's Note

Springer Nature remains neutral with regard to jurisdictional claims in published maps and institutional affiliations.

Ready to submit your research? Choose BMC and benefit from:

- fast, convenient online submission
- thorough peer review by experienced researchers in your field
- rapid publication on acceptance
- support for research data, including large and complex data types
- gold Open Access which fosters wider collaboration and increased citations
- maximum visibility for your research: over 100M website views per year

At BMC, research is always in progress.

Learn more biomedcentral.com/submissions

